

LIGHTFUSION: A LIGHT-WEIGHTED, DOUBLE FUSION FRAMEWORK FOR UNIFIED MULTIMODAL UNDERSTANDING AND GENERATION

Zeyu Wang^{1*} Zilong Chen^{2,4*} Chenhui Gou^{3,4*} Feng Li⁴ Chaorui Deng⁴
 Deyao Zhu⁴ Kunchang Li⁴ Weihao Yu⁴ Haoqin Tu¹ Haoqi Fan⁴ Cihang Xie¹

¹UC Santa Cruz ²Tsinghua University ³Monash University ⁴ByteDance Seed

Project Page: <https://ucsc-vlaa.github.io/LightFusion/>

ABSTRACT

Unified multimodal models have recently shown remarkable gains in both capability and versatility, yet most leading systems are still trained from scratch and require substantial computational resources. In this paper, we show that competitive performance can be obtained far more efficiently by *strategically* fusing publicly available models specialized for either generation or understanding. Our key design is to retain the original blocks while additionally interleaving multimodal self-attention blocks throughout the networks. This *double fusion mechanism* (1) effectively enables rich multi-modal fusion while largely preserving the original strengths of the base models, and (2) catalyzes synergistic fusion of high-level semantic representations from the understanding encoder with low-level spatial signals from the generation encoder. By training with only $\sim 35\text{B}$ tokens, this approach achieves strong results across multiple benchmarks: 0.91 on GenEval for compositional text-to-image generation, 82.16 on DPG-Bench for complex text-to-image generation, 6.06 on GEditBench, and 3.77 on ImgEdit-Bench for image editing. By fully releasing the entire suite of code, model weights, and datasets, we hope to support future research on unified multimodal modeling.

1 INTRODUCTION

In recent years, multimodal learning has witnessed a notable transition from specialized models to a new generation of unified multimodal models (UMMs). The central innovation of these models lies in their ability to natively couple language and vision, enabling them to understand both modalities and to generate text and images within a single, end-to-end modeling stack. Production-scale systems such as GPT-4o (Hurst et al., 2024) and Gemini 2.0 Flash (Google, 2025) have further demonstrated the promise of this paradigm, with impressive prompt adherence and dialogue-based image generation and manipulation capabilities, highlighting the potential of “any-to-any” paradigm.

Meanwhile, there is also a growing push inside the open-source research community to advance UMMs. The early works (Team, 2024; Wang et al., 2024; Zhou et al., 2024; Wu et al., 2025a; Chen et al., 2025c) adopt a single-stack transformer over mixed-modality sequences, but jointly optimizing autoregressive and diffusion objectives introduces fundamental training conflicts. Subsequent works (Deng et al., 2025; Wu et al., 2025b; Wang et al., 2025b; Wei et al., 2025) decouples understanding and generation into separate pathways, easing optimization and improving performance, yet requiring large-scale training and substantial compute that limit accessibility.

Recent attempts to build UMMs efficiently—such as lightweight connectors that map final-layer representations from pretrained vision–language models (VLMs, *i.e.*, used for understanding) to diffusion transformers (DiTs, *i.e.*, used for generation) for conditional generation (Pan et al., 2025; Chen et al., 2025a; Lin et al., 2025)—are promising but remain incomplete, as performance and task generality are still limited.

*Equal contribution.

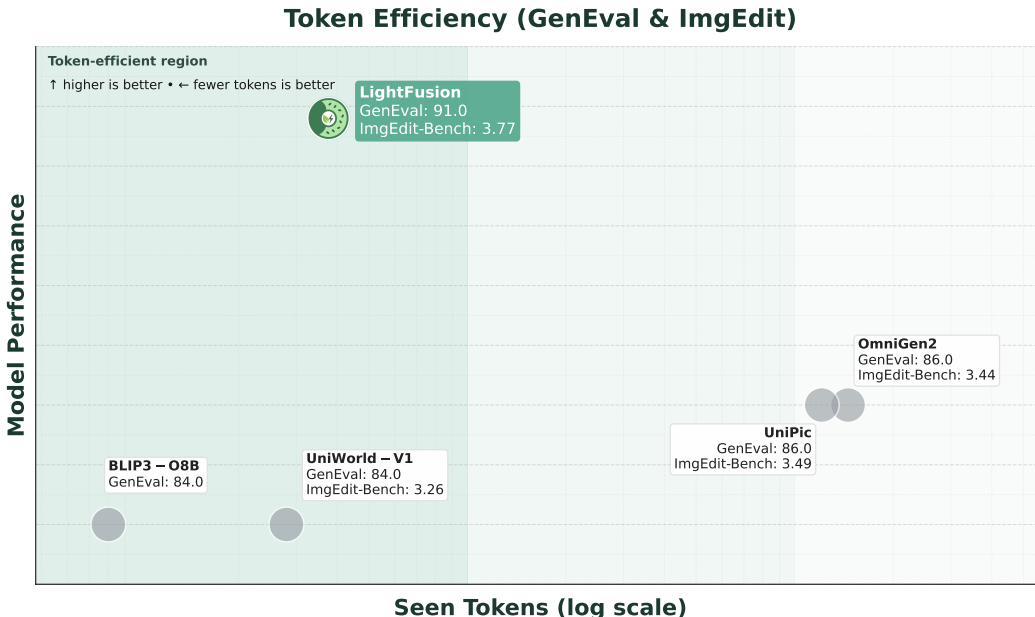


Figure 1: Token efficiency comparison on T2I and image editing benchmarks. Our LightFusion outperforms many leading unified models that uses significantly more tokens for training, showing great token efficiency. Note that we use our best estimate for the number of seen tokens of OmniGen2 and UniPic since their original training recipe is unclear to the public.

This work continues the pursuit of efficient UMM construction by introducing a novel and powerful fusion strategy. At the core of our approach is a mechanism that tightly couples the VLM and DiT blocks of strong base models through zero-initialized multimodal self-attention layers. This design keeps the strong autoregressive and diffusion capabilities of the base models while enabling early, deep, and continuous cross-modal interaction. Through controlled studies, we show that this strategy substantially outperforms the widely adopted “Shallow Fusion” approach (Tang et al., 2025), which conditions the generator only on the final-layer output of the understanding branch (Chen et al., 2025a; Lin et al., 2025; Wu et al., 2025b). Furthermore, our design maintains two coordinated pathways that cleanly separate ViT tokens from VAE latents, allowing the model to naturally integrate high-level semantics with low-level visual signals. This synergy leads to more accurate, consistent, and faithful image editing behaviors.

We refer to this architecture as *Double Fusion*, highlighting its dual role in simultaneously bridging (i) the understanding and generation branches and (ii) ViT-based and VAE-based visual representations. Together, these components enable efficient training and deliver strong performance while requiring substantially fewer tokens and compute than prior works, as illustrated in Figure 1. The resulting model, which we call *LightFusion*, is lightweight and modular, making it suitable for a wide range of applications and research settings.

LightFusion delivers state-of-the-art results across multiple benchmarks, including a GenEval score of 0.91 for compositional text-to-image generation, a DPG-Bench score of 82.16 for complex text-to-image generation, and scores of 6.06 on GEditBench and 3.77 on ImgEdit-Bench for image editing. Remarkably, trained on only ~35B seen tokens, LightFusion achieves performance on par with, or even surpassing, leading models like UniPic and OmniGen2, which were trained with orders of magnitude more tokens. These results highlight LightFusion’s efficiency and suggest new directions for the design of future UMM architectures.

2 RELATED WORKS

Text-to-Image Generation. Diffusion models (Ho et al., 2020; Song et al., 2020) have emerged as the dominant paradigm for open-domain image synthesis, surpassing GANs (Goodfellow et al., 2020) with improved stability and semantic fidelity. Seminal works, such as Stable Diffusion and

its successors (Rombach et al., 2022; Podell et al., 2023; Esser et al., 2024), DALL·E (Ramesh et al., 2022), and Imagen (Imagen 3 Team, 2024), demonstrated the power of large-scale pretraining and latent denoising for high-resolution, text-aligned generation. More recently, flow-matching models (Lipman et al., 2022) have been proposed as a powerful alternative to diffusion, modeling vector fields between noise and data distributions, and have achieved strong results in large-scale systems (Labs, 2024; Wan et al., 2025).

Image Editing. Image editing has been widely studied as an extension of text-to-image generation. InstructPix2Pix (Brooks et al., 2023) pioneered the supervised paradigm based on $\{instruction, source\ image, target\ image\}$ triplets. Subsequent works improved this approach by diversifying training data and improving quality (Zhang et al., 2023; Hui et al., 2025; Wei et al., 2024; Ye et al., 2025), or by incorporating stronger control signals (Tan et al., 2023; Liu et al., 2025; Zhang et al., 2025). More recent frameworks such as OmniGen (Xiao et al., 2025) and UniReal (Chen et al., 2025b) unify common image generation tasks by processing various conditional inputs with modified attention mechanisms, demonstrating the potential of a single model for multiple generation tasks.

Unified Multimodal Models. UMMs have rapidly gained attention for their ability to support both understanding and generation, exhibiting strong generalization across visual understanding, generation, editing, and many other downstream tasks. Early UMM works (Team, 2024; Wang et al., 2024; Zhou et al., 2024; Wu et al., 2025a; Chen et al., 2025c; Xie et al., 2024) employed a single Transformer backbone to process interleaved image and text tokens. Subsequent work introduced separate understanding and generation branches, yielding improved performance while easing optimization towards two distinct tasks (Shi et al., 2024; Deng et al., 2025; Wu et al., 2025b; Wei et al., 2025). Nonetheless, these models generally depend on extensive large-scale pre-training over massive image-text corpora, which constrains their accessibility and limit the broader exploration of UMM researches.

Another line of works, such as BLIP3-o (Chen et al., 2025a), MetaQueries (Pan et al., 2025) and UniWorld (Lin et al., 2025), aims to build UMMs efficiently by coupling frozen multimodal LLMs with trainable diffusion decoders. Yet, existing schemes typically rely on shallow or late-stage fusion, restricting the expressiveness and depth of cross-modal alignment.

Our LightFusion model advances this direction through a double-fusion architecture. It tightly couples a powerful VLM with a DiT-based generator, enabling information to flow richly across modalities. This dual pathway design also naturally and effectively integrates high-level ViT features with low-level VAE latents, yielding a more coherent and semantically grounded generation pipeline.

Notably, the double-fusion structure bears similarity to the modality-specialized mixture-of-experts designs in LMFusion (Shi et al., 2024) and BAGEL (Deng et al., 2025), with drastically different underlying requirements. Those models initialize the generation branch with duplicated LLM weights, demanding orders of magnitude more seen tokens and extensive private training data. In contrast, LightFusion trains publicly available fused base models with only public data, achieving strong performance in an extremely lightweight and accessible training regime.

3 METHODS

3.1 MODEL ARCHITECTURE

The core design of LightFusion is a Double Fusion mechanism. Specifically, as illustrated in Figure 2, this design interleaves multimodal self-attention blocks across VLM (used for understanding) and DiT (used for generation) blocks. To fully leverage the strength of open-source models with extensive pre-training and post-training, we employ QWen2.5-VL-7B (Bai et al., 2025) for the understanding pathway and Wan2.2-TI2V-5B (Wan et al., 2025) for the generation pathway. Note that given QWen2.5-VL-7B has slightly fewer layers than Wan2.2-TI2V-5B (two layers fewer), its final-layer output is reused as input to the last two multimodal self-attention blocks.

In this design, the VLM blocks process understanding tokens (*i.e.*, text and ViT tokens), while the DiT blocks operate on generation tokens (*i.e.*, VAE tokens). The multimodal self-attention blocks span all token types, enabling rich cross-modal interactions. To facilitate this, we adopt the generalized causal attention mechanism from BAGEL (Deng et al., 2025), allowing tokens from different modalities and tokenizers to attend to one another. Importantly, each multimodal self-attention block is zero-

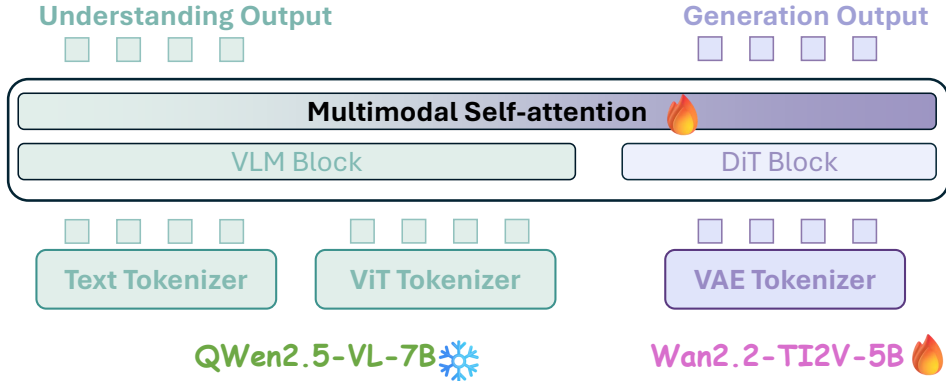


Figure 2: Overview of the LightFusion architecture. Text and ViT tokens (understanding pathway) and VAE tokens (generation pathway) are processed by pre-trained VLM and DiT blocks, respectively. At each layer, a zero-initialized multimodal self-attention module enables cross-modal interactions without altering the original model architectures.

initialized, ensuring that the feature distributions of the VLM and DiT remain intact at the start of training, thereby preserving their strong autoregressive and denoising capabilities. For image editing tasks, both ViT and VAE tokens are extracted from the source image and provided as conditioning signals. The ViT tokens are extracted using the QWen2.5-VL vision encoders. The VAE tokens are extracted by the 3D causal VAE from Wan2.2-TI2V-5B (Wan et al., 2025), which provides 16× spatial compression and 4× temporal compression.

We expect this design offer several key advantages:

- **Seamless model integration.** The framework incorporates powerful pre-trained VLM and DiT models without altering their architectures, offering a straightforward and generalizable method for fusing publicly available models into a unified multimodal system. In line with prior findings (Tang et al., 2025), we observe that this “deep fusion” strategy consistently outperforms “shallow fusion” approaches while delivering superior token efficiency.
- **Dual-pathway visual representation.** By naturally integrating ViT tokens (high-level semantics) and VAE tokens (low-level signals), the architecture achieves precise and consistent image editing, effectively balancing global understanding with fine-grained detail.
- **Information-preserving multimodal interaction.** Leveraging hidden states from all understanding and generation layers within the multimodal self-attention avoids compressing conditioning inputs into a fixed-length representation (Pan et al., 2025; Chen et al., 2025a; Wei et al., 2025), ensuring rich, loss-free cross-modal interactions.

3.2 DATASET

Our training corpus comprises ~45 million samples, encompassing both text-to-image generation and image-editing tasks. We source data from publicly available datasets, including BLIP-3o (Chen et al., 2025a), Civitai (civ, 2024), OmniGen (Xiao et al., 2025), OmniEdit (Wei et al., 2024), GPT-IMAGE-EDIT-1.5M (Wang et al., 2025c), and UniWorld-V1 (Lin et al., 2025), supplemented by a synthetic self-curated dataset of ~4.5 million samples. Notably, we apply a VLM to refine the editing instructions of public image editing data conditioned on source–target pairs, thereby enhancing instruction precision.

3.3 TRAINING

We adopt NaViT-style image processing to preserve native aspect ratios (Dehghani et al., 2023), constraining inputs to a minimum short side of 512 pixels and a maximum long side of 1024 pixels, thereby improving generation quality. ViT tokens are extracted from input sizes ranging from a minimum short side of 224 pixels to a maximum long side of 532 pixels. The LightFusion model is trained for 70K steps using the AdamW optimizer, with 2K warmup steps and a fixed learning rate

Table 1: Comparison of different models across understanding, generation, editing, and in-context Generation tasks. † refers to the methods using LLM rewriter. For UMMS, ★☆☆ refers to only model checkpoints and evaluation code being released; ★★☆☆ refers to only model checkpoints and training/evaluation code being released; ★★★ refers to the full suite of all the {model, data, code} being released.

| Model | # Params | Openness | Understanding | | | Image Generation | | Image Editing | |
|-----------------------|--------------|----------|---------------|------|--------|------------------|-------|---------------|----------|
| | | | MMB | MMMU | MM-Vet | GenEval | DPG | ImgEdit | GEdit-EN |
| LLaVA-1.5 | – | – | 36.4 | 67.8 | 36.3 | – | – | – | – |
| LLaVA-NeXT | – | – | 79.3 | 51.1 | 57.4 | – | – | – | – |
| SDXL | – | – | – | – | – | 0.55 | 74.7 | – | – |
| SD3-medium | – | – | – | – | – | 0.62 | 84.1 | – | – |
| FLUX.1-dev | – | – | – | – | – | 0.66 | 84.0 | – | – |
| Instruct-P2P | – | – | – | – | – | – | – | 1.88 | 3.68 |
| MagicBrush | – | – | – | – | – | – | – | 1.90 | 1.86 |
| AnyEdit | – | – | – | – | – | – | – | 2.45 | 3.21 |
| Step1X-Edit | – | – | – | – | – | – | – | 3.06 | 6.70 |
| IC-Edit | – | – | – | – | – | – | – | 3.05 | 4.84 |
| <i>Unified models</i> | | | | | | | | | |
| Janus-Pro | – | ★☆☆ | 75.5 | 36.3 | 39.8 | 0.80 | 84.19 | – | – |
| Emu3 | – | ★☆☆ | 58.5 | 31.6 | 37.2 | 0.66† | 80.60 | – | – |
| UniPic | 1.5B | ★☆☆ | – | – | – | 0.86 | 85.50 | 3.49 | 5.83 |
| UniPic 2.0 | 7B + 2B | ★☆☆ | 83.5 | 58.6 | 67.1 | 0.90† | 83.79 | 4.06 | 7.10 |
| Ovis-U1 | 2.4B + 1.2B | ★☆☆ | 77.8 | 51.1 | 66.7 | 0.89 | 83.72 | 4.00 | 6.42 |
| MetaQuery-XL | 7B + 1.6B | ★★☆ | 83.5 | 58.6 | 66.6 | 0.80† | 82.05 | – | – |
| Show-o2 | 7B | ★★☆ | 79.3 | 48.9 | – | 0.76 | 86.14 | – | – |
| OmniGen | 3.8B | ★★☆ | – | – | – | 0.68 | 81.16 | 2.96 | 5.06 |
| OmniGen2 | 3B + 4B | ★★☆ | 79.1 | 53.1 | 61.8 | 0.86† | 83.57 | 3.44 | 6.42 |
| BAGEL | 7B + 7B | ★★☆ | 85.0 | 55.3 | 67.2 | 0.88† | 85.07 | 3.20 | 6.52 |
| BLIP3-o 4B | 3B + 1.4B | ★★★ | 78.6 | 46.6 | 60.1 | 0.81† | 79.36 | – | – |
| BLIP3-o 8B | 7B + 1.4B | ★★★ | 83.5 | 58.6 | 66.6 | 0.84† | 81.60 | – | – |
| UniWorld-V1 | 7B + 12B | ★★★ | 83.5 | 58.6 | 67.1 | 0.84† | 81.38 | 3.26 | 4.85 |
| LightFusion | 7B + 5B + 3B | ★★★ | 83.5 | 58.6 | 67.1 | 0.91† | 82.16 | 3.77 | 6.06 |

of 0.00003. The sequence length is configured between 16,384 (minimum) and 20,480 (maximum) tokens. To enable classifier-free guidance, text tokens, VAE tokens, and ViT tokens are randomly dropped with probabilities of 0.1, 0.1, and 0.5, respectively. The understanding branch is frozen during the entire training time to preserve the strong understanding ability of QWen2.5-VL-7B.

We divide the full training process into three stages. In the first stage, a large proportion of common T2I data and a small proportion of high-quality T2I and editing data are used. In the second and third stages, we progressively increase the ratios of high-quality T2I and editing data, respectively. In practice, this staged setup proves beneficial for improving both text-to-image generation and image-editing performance.

4 EXPERIMENTS

In this section, we evaluate the performance of LightFusion across a diverse set of image understanding, generation, and editing tasks. Sec. 4.1 presents the visual understanding results. Text-to-image generation results are reported in Sec. 4.2, followed by a focus on image editing in Sec. 4.3. Sec. 4.4 presents our ablation study, analyzing key design choices of the model. Our experiment results show that LightFusion efficiently achieves strong performances over a wide spectrum of tasks and benchmarks, demonstrating the efficacy of our double fusion approach.

4.1 VISUAL UNDERSTANDING

By freezing the understanding branch, our model preserves the strong multimodal reasoning capabilities of the pre-trained QWen2.5-VL-7B. As reported in Table 1, LightFusion attains competitive performances of 83.5 on MMBench (Liu et al., 2024), 58.6 on MMMU (Yue et al., 2024), and 67.1 on MM-Vet (Yu et al., 2023). This architectural choice aligns with recent state-of-the-art designs, such as UniWorld-V1 (Lin et al., 2025), OmniGen2 (Wu et al., 2025b), and UniPic 2.0 (Wang et al., 2025b),



Figure 3: Qualitative text-to-image results from LightFusion, showcasing high-quality generations with strong fidelity to text prompts and consistent rendering across diverse aspect ratios.

which similarly prioritize maintaining robust understanding performance. As a result, LightFusion effectively mitigates potential degradation in understanding capabilities and surpasses several strong competitors, including Ovis-U1 (Wang et al., 2025a), Show-o2 (Xie et al., 2025), and Janus-Pro (Chen et al., 2025c).

4.2 TEXT-TO-IMAGE GENERATION

We test on widely recognized benchmarks, GenEval and DPG-Bench, to evaluate LightFusion’s text-to-image generation performance. These benchmarks primarily assess the model’s capabilities in compositional image generation and dense prompt following, respectively. In addition, we provide qualitative visualization examples in Figure 3. Both the quantitative results and qualitative illustrations demonstrate that LightFusion is capable of producing high-fidelity, aesthetically compelling images.

GenEval. As reported in Table 2, LightFusion attains an overall score of 0.91 on GenEval when evaluated with LLM-rewritten prompts, highlighting its strong compositional understanding across diverse generative tasks. This performance surpasses several competitive baselines, including UniPiC (0.86), OmniGen2 (0.86), BAGEL (0.88) and UniPiC2.0 (0.90). Notably, LightFusion is trained with over an order of magnitude of less seen tokens, underscoring its remarkable efficiency in terms of both data and compute resources.

DPG-Bench. As reported in Table 3, on DPG-Bench, LightFusion achieves an overall score of 82.16, demonstrating competitive performance in long-prompt adherence and complex scene generation. This result surpasses other strong unified models such as BLIP3-o 8B (81.60) and UniWorld-V1 (81.38). Additionally, detailed breakdowns in Table 3 indicate that LightFusion maintains consistently strong performance across multiple dimensions of evaluation, including global coherence, entity recognition, attribute understanding, and relational reasoning.

Table 2: Evaluation of text-to-image generation ability on GenEval benchmark. † refers to the methods using LLM rewriter.

| Method | Single object† | Two object† | Counting† | Colors† | Position† | Color attribution† | Overall† |
|---------------|----------------|-------------|-----------|---------|-----------|--------------------|----------|
| SDv2.1 | 0.98 | 0.51 | 0.44 | 0.85 | 0.07 | 0.17 | 0.50 |
| SDXL | 0.96 | 0.74 | 0.39 | 0.85 | 0.15 | 0.23 | 0.55 |
| IF-XL | 0.97 | 0.74 | 0.66 | 0.81 | 0.13 | 0.35 | 0.61 |
| LUMINA-Next | 0.92 | 0.46 | 0.48 | 0.70 | 0.09 | 0.13 | 0.46 |
| SD3-medium | 0.99 | 0.94 | 0.72 | 0.89 | 0.33 | 0.60 | 0.74 |
| FLUX.1-dev | 0.99 | 0.81 | 0.79 | 0.74 | 0.20 | 0.47 | 0.67 |
| NOVA | 0.99 | 0.91 | 0.62 | 0.85 | 0.33 | 0.56 | 0.71 |
| OmniGen | 0.98 | 0.84 | 0.66 | 0.74 | 0.40 | 0.43 | 0.68 |
| TokenFlow-XL | 0.95 | 0.60 | 0.41 | 0.81 | 0.16 | 0.24 | 0.55 |
| Janus | 0.97 | 0.68 | 0.30 | 0.84 | 0.46 | 0.42 | 0.61 |
| Janus Pro | 0.99 | 0.89 | 0.59 | 0.90 | 0.79 | 0.66 | 0.80 |
| Emu3-Gen† | 0.99 | 0.81 | 0.42 | 0.80 | 0.49 | 0.45 | 0.66 |
| Show-o2† | 1.00 | 0.87 | 0.58 | 0.92 | 0.52 | 0.62 | 0.76 |
| MetaQuery-XL† | - | - | - | - | - | - | 0.80 |
| UniPic | 0.98 | 0.92 | 0.74 | 0.91 | 0.89 | 0.72 | 0.86 |
| UniPic 2.0† | - | - | - | - | - | - | 0.90 |
| Ovis-U1† | 0.98 | 0.98 | 0.90 | 0.92 | 0.79 | 0.75 | 0.89 |
| BAGEL† | 0.98 | 0.95 | 0.84 | 0.95 | 0.78 | 0.77 | 0.88 |
| OmniGen2† | 0.99 | 0.96 | 0.74 | 0.98 | 0.71 | 0.75 | 0.86 |
| BLIP3-o† 8B | - | - | - | - | - | - | 0.84 |
| UniWorld-V1† | 0.98 | 0.93 | 0.81 | 0.89 | 0.74 | 0.71 | 0.84 |
| LightFusion† | 1.00 | 0.97 | 0.93 | 0.94 | 0.79 | 0.81 | 0.91 |

Table 3: Evaluation of text-to-image generation ability on DPG-Bench benchmark.

| Method | Global† | Entity† | Attribute† | Relation† | Other† | Overall† |
|----------------|---------|---------|------------|-----------|--------|----------|
| LUMINA-Next | 82.82 | 88.65 | 86.44 | 80.53 | 81.82 | 74.63 |
| SDXL | 83.27 | 82.43 | 80.91 | 86.76 | 80.41 | 74.65 |
| PlayGroundv2.5 | 83.06 | 82.59 | 81.20 | 84.08 | 83.50 | 75.47 |
| Hunyuan-DiT | 84.59 | 80.59 | 88.01 | 74.36 | 86.41 | 78.87 |
| PixArt-Σ | 86.89 | 82.89 | 88.94 | 86.59 | 87.68 | 80.54 |
| DALLE3 | 90.97 | 89.61 | 88.39 | 90.58 | 89.83 | 83.50 |
| SD3-medium | 87.90 | 91.01 | 88.83 | 80.70 | 88.68 | 84.08 |
| FLUX.1-dev | 82.10 | 89.50 | 88.70 | 91.10 | 89.40 | 84.00 |
| OmniGen | 87.90 | 88.97 | 88.47 | 87.95 | 83.56 | 81.16 |
| TokenFlow-XL | 78.72 | 79.22 | 81.29 | 85.22 | 71.20 | 73.38 |
| Janus | 82.33 | 87.38 | 87.70 | 85.46 | 86.41 | 79.68 |
| Janus Pro | 86.90 | 88.90 | 89.40 | 89.32 | 89.02 | 84.19 |
| Show-o2 | 89.00 | 91.78 | 89.96 | 91.81 | 91.64 | 86.14 |
| EMU3 | 85.21 | 86.68 | 86.84 | 90.22 | 83.15 | 80.60 |
| UniPic | 89.65 | 87.78 | 90.84 | 91.89 | 91.95 | 85.50 |
| UniPic 2.0 | - | - | - | - | - | 83.79 |
| Ovis-U1 | 82.37 | 90.08 | 88.68 | 93.35 | 85.20 | 83.72 |
| BAGEL | 88.94 | 90.37 | 91.29 | 90.82 | 88.67 | 85.07 |
| OmniGen2 | 88.81 | 88.83 | 90.18 | 89.37 | 90.27 | 83.57 |
| BLIP3-o 8B | - | - | - | - | - | 81.60 |
| UniWorld-V1 | 83.64 | 88.39 | 88.44 | 89.27 | 87.22 | 81.38 |
| LightFusion | 87.13 | 89.59 | 87.58 | 90.22 | 90.44 | 82.16 |

4.3 IMAGE EDITING

We evaluate LightFusion’s image editing capabilities using two widely adopted benchmarks: GEdit-Bench-EN (Liu et al., 2025) and ImgEdit-Bench (Ye et al., 2025). GEdit-Bench-EN consists of real-world user editing instances, while ImgEdit-Bench encompasses nine distinct editing tasks (e.g., add, remove, alter). We further provide qualitative examples of LightFusion’s editing results in Figure 4. Both quantitative and qualitative results demonstrate that LightFusion delivers strong performance in instruction-based image editing, excelling in both editing accuracy and content preservation.

GEdit-Bench-EN. As shown in Table 4, LightFusion achieves an overall score of 6.06, positioning it among the top-tier unified models. The model demonstrates particular strength in semantic consistency (SC), attaining a score of 6.34, which reflects robust instruction-following capabilities.

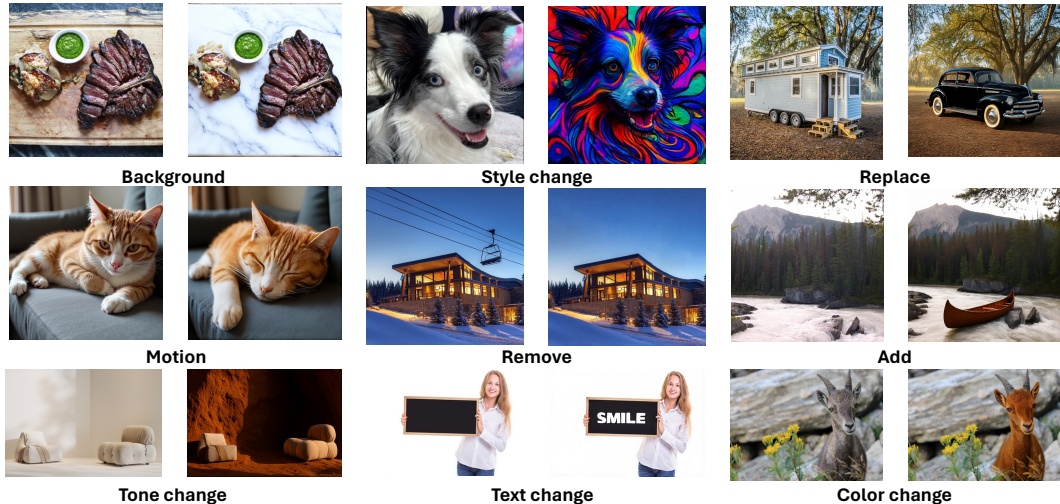


Figure 4: Qualitative image editing results generated by LightFusion. The model exhibits strong instruction following and content preservation capability across a diverse range of editing tasks.

Table 4: Evaluation of image editing ability on GEdit-Bench-EN

| Model | SC \uparrow | PQ \uparrow | Overall \uparrow |
|------------------|---------------|---------------|--------------------|
| Gemini-2.0-flash | 6.73 | 6.61 | 6.32 |
| GPT-4o | 7.85 | 7.62 | 7.53 |
| Instruct-Pix2Pix | 3.58 | 5.49 | 3.68 |
| MagicBrush | 4.68 | 5.66 | 4.52 |
| AnyEdit | 3.18 | 5.82 | 3.21 |
| ICEdit | 5.11 | 6.85 | 4.84 |
| Step1X-Edit | 7.09 | 6.76 | 6.70 |
| OmniGen2 | 7.16 | 6.77 | 6.41 |
| BAGEL | 7.36 | 6.83 | 6.52 |
| Ovis-U1 | – | – | 6.42 |
| UniPic | 6.72 | 6.18 | 5.83 |
| UniPic 2.0 | – | – | 7.10 |
| UniWorld-V1 | 4.93 | 7.43 | 4.85 |
| LightFusion | 6.34 | 7.31 | 6.06 |

This result notably surpasses that of UniWorld-V1 (4.93) by a large margin, underscoring the effectiveness of our hybrid ViT+VAE feature fusion strategy compared to only using ViT tokens as condition in image editing task.

ImgEdit-Bench. As can be seen in Table 5, LightFusion achieves an overall score of 3.77, outperforming other strong open-source competitors such as UniWorld-V1 (3.26) and OmniGen2 (3.44). Importantly, LightFusion ranks first among open-source models in several key categories, including Add (4.21), Replace (4.55), Remove (3.80), and Hybrid (3.92), which highlights the model’s robust and consistent editing ability across a broad spectrum of tasks.

4.4 ABLATION STUDY

For ablation study experiments, we keep the general training setup for the *“Deep Fusion vs Shallow Fusion”* study, while opt for 40K training steps for the others for faster experiment cycles.

Deep Fusion vs Shallow Fusion. Previous efficient UMM approaches typically employ a lightweight connector that maps the final output of the understanding branch as a conditional input to the

Table 5: Evaluation of image editing ability on ImgEdit-Bench.

| Model | Add | Adjust | Extract | Replace | Remove | Background | Style | Hybrid | Action | Overall |
|------------------|------|--------|---------|---------|--------|------------|-------|--------|--------|---------|
| GPT-4o | 4.61 | 4.33 | 2.90 | 4.35 | 3.66 | 4.57 | 4.93 | 3.96 | 4.89 | 4.20 |
| MagicBrush | 2.84 | 1.58 | 1.51 | 1.97 | 1.58 | 1.75 | 2.38 | 1.62 | 1.22 | 1.90 |
| Instruct-Pix2Pix | 2.45 | 1.83 | 1.41 | 2.01 | 1.44 | 1.44 | 3.55 | 1.20 | 1.46 | 1.88 |
| AnyEdit | 3.18 | 2.95 | 1.14 | 2.49 | 2.21 | 2.88 | 3.82 | 1.56 | 2.65 | 2.45 |
| UltraEdit | 3.44 | 2.81 | 2.00 | 2.96 | 2.45 | 2.83 | 3.76 | 1.91 | 2.98 | 2.70 |
| Step1X-Edit | 3.88 | 3.41 | 1.76 | 3.40 | 2.83 | 3.16 | 6.63 | 2.52 | 2.52 | 3.06 |
| ICEdit | 3.58 | 3.39 | 1.73 | 3.15 | 2.93 | 3.08 | 3.84 | 2.04 | 3.68 | 3.05 |
| OmniGen2 | 3.74 | 3.54 | 1.77 | 3.21 | 2.77 | 3.57 | 4.81 | 2.30 | 4.14 | 3.43 |
| BAGEL | 3.56 | 3.31 | 1.88 | 2.62 | 2.88 | 3.44 | 4.49 | 2.38 | 4.17 | 3.20 |
| Ovis-U1 | 4.12 | 3.92 | 2.36 | 4.09 | 3.57 | 4.22 | 4.69 | 3.23 | 3.61 | 3.98 |
| UniPic | 3.66 | 3.51 | 2.06 | 4.31 | 2.77 | 3.77 | 4.76 | 2.56 | 4.04 | 3.49 |
| UniPic 2.0 | - | - | - | - | - | - | - | - | - | 4.06 |
| UniWorld-V1 | 3.82 | 3.66 | 2.31 | 3.45 | 3.02 | 2.99 | 4.71 | 2.96 | 2.74 | 3.26 |
| LightFusion | 4.21 | 3.23 | 1.83 | 4.55 | 3.80 | 4.15 | 4.66 | 3.93 | 3.60 | 3.77 |

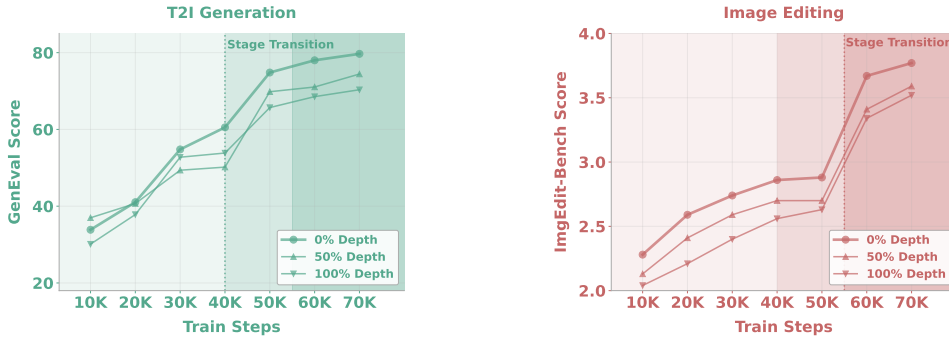


Figure 5: Deep fusion vs. shallow fusion design choices. Regions of different colors represent different training stages. The “0% Depth” deep fusion approach in our LightFusion consistently outperforms other options.

generation branch. In contrast, our Double Fusion design allows language and visual tokens to interact from the earliest layers, enabling deeper and more continuous cross-modal integration.

To systematically compare the two strategies, we vary the depth at which features from the VLM are injected into the generation pathway. Specifically, “0% Depth” denotes the case where the i -th DiT block is conditioned on the i -th VLM block’s output. When the VLM blocks are exhausted, the final VLM output is repeated as input for the remaining DiT blocks. Conversely, “100% Depth” corresponds to conditioning all DiT blocks exclusively on the final VLM output, effectively repeating it across all multimodal self-attention layers. Importantly, we keep the total number of multimodal self-attention layers fixed, ensuring identical parameter counts and a fair comparison.

As shown in Figure 5, the “0% Depth” option—adopted in our LightFusion model—consistently outperforms shallow or early-layer fusion for both text-to-image and image-editing tasks. We attribute this advantage to the fact that the final VLM representations encode high-level semantics more suitable for next-token prediction rather than multimodal alignment.

Visual Tokenizer Choices. VAE and ViT encoders provide complementary visual representations: VAEs emphasize low-level details, while ViTs capture high-level semantic information. To assess which type of information is more suitable for image editing, we conduct an ablation study on visual tokenizer choice, with results reported in Table 6a. The findings indicate that both sources of information are essential—combining low-level details with high-level semantics leads to more consistent and accurate image editing outcomes.

Training Timestep Shift. Shifting timesteps during inference has been shown to improve generation quality in state-of-the-art models (Labs, 2024; Wan et al., 2025). In our preliminary experiments, we observe that the strong base DiT pathway already demonstrates robust denoising capabilities. Building on this, and following the inference-time timestep shifting strategy (Labs, 2024; Wan et al., 2025), we increase the training diffusion timestep range from 1.0 to 4.0 to achieve more noisy

Table 6: Ablation study on visual tokenizer and timestep shift choices.

| Encoder | GEEdit-EN | ImgEdit |
|-----------|-----------|---------|
| ViT | 3.91 | 2.65 |
| VAE | 4.93 | 3.38 |
| ViT + VAE | 5.61 | 3.57 |

(a) Evaluation of different visual tokenizer choices.

| Timestep Shift | DPG-Bench | ImgEdit |
|----------------|-----------|---------|
| 1 | 76.67 | 3.07 |
| 2 | 78.84 | 3.36 |
| 4 | 81.77 | 3.57 |

(b) Evaluation of different timestep shift choices.

corrupted samples. As reported in Table 6b, a timestep shift larger than 1 consistently lead to better results.

5 CONCLUSION

This work introduces LightFusion, a unified multimodal model for both understanding and generation that achieves state-of-the-art performance across diverse tasks while requiring substantially fewer training tokens and compute than prior leading UMMs. These advantages are largely benefited by our Double Fusion design, which enables effective cross-modal feature interactions and naturally integrates high-level semantics with low-level visual details. By releasing the entire suite of code, models, and data, we hope to support reproducibility and accelerate progress in unified multimodal modeling.

REFERENCES

- Civitai. 2024. URL <https://civitai.com/>.
- Shuai Bai, Keqin Chen, Xuejing Liu, Jialin Wang, Wenbin Ge, Sibao Song, Kai Dang, Peng Wang, Shijie Wang, Jun Tang, et al. Qwen2. 5-vl technical report. *arXiv preprint arXiv:2502.13923*, 2025.
- Tim Brooks, Aleksander Holynski, and Alexei A Efros. Instructpix2pix: Learning to follow image editing instructions. In *Proceedings of the IEEE/CVF conference on computer vision and pattern recognition*, pp. 18392–18402, 2023.
- Jiuhai Chen, Zhiyang Xu, Xichen Pan, Yushi Hu, Can Qin, Tom Goldstein, Lifu Huang, Tianyi Zhou, Saining Xie, Silvio Savarese, et al. Blip3-o: A family of fully open unified multimodal models-architecture, training and dataset. *arXiv preprint arXiv:2505.09568*, 2025a.
- Xi Chen, Zhifei Zhang, He Zhang, Yuqian Zhou, Soo Ye Kim, Qing Liu, Yijun Li, Jianming Zhang, Nanxuan Zhao, Yilin Wang, et al. Unireal: Universal image generation and editing via learning real-world dynamics. In *Proceedings of the Computer Vision and Pattern Recognition Conference*, pp. 12501–12511, 2025b.
- Xiaokang Chen, Zhiyu Wu, Xingchao Liu, Zizheng Pan, Wen Liu, Zhenda Xie, Xingkai Yu, and Chong Ruan. Janus-pro: Unified multimodal understanding and generation with data and model scaling. *arXiv preprint arXiv:2501.17811*, 2025c.
- Mostafa Dehghani, Basil Mustafa, Josip Djolonga, Jonathan Heek, Matthias Minderer, Mathilde Caron, Andreas Steiner, Joan Puigcerver, Robert Geirhos, Ibrahim M Alabdulmohsin, et al. Patch n’pack: Navit, a vision transformer for any aspect ratio and resolution. *Advances in Neural Information Processing Systems*, 36:2252–2274, 2023.
- Chaorui Deng, Deyao Zhu, Kunchang Li, Chenhui Gou, Feng Li, Zeyu Wang, Shu Zhong, Weihao Yu, Xiaonan Nie, Ziang Song, et al. Emerging properties in unified multimodal pretraining. *arXiv preprint arXiv:2505.14683*, 2025.
- Patrick Esser, Sumith Kulal, Andreas Blattmann, Rahim Entezari, Jonas Müller, Harry Saini, Yam Levi, Dominik Lorenz, Axel Sauer, Frederic Boesel, et al. Scaling rectified flow transformers for high-resolution image synthesis. In *Forty-first international conference on machine learning*, 2024.

- Ian Goodfellow, Jean Pouget-Abadie, Mehdi Mirza, Bing Xu, David Warde-Farley, Sherjil Ozair, Aaron Courville, and Yoshua Bengio. Generative adversarial networks. *Communications of the ACM*, 63(11):139–144, 2020.
- Google. Gemini 2.0 flash. 2025. URL <https://developers.googleblog.com/en/the-next-chapter-of-the-gemini-era-for-developers/>.
- Jonathan Ho, Ajay Jain, and Pieter Abbeel. Denoising diffusion probabilistic models. *Advances in neural information processing systems*, 33:6840–6851, 2020.
- Mude Hui, Siwei Yang, Bingchen Zhao, Yichun Shi, Heng Wang, Peng Wang, Cihang Xie, and Yuyin Zhou. HQ-edit: A high-quality dataset for instruction-based image editing. In *The Thirteenth International Conference on Learning Representations*, 2025.
- Aaron Hurst, Adam Lerer, Adam P Goucher, Adam Perelman, Aditya Ramesh, Aidan Clark, AJ Ostrow, Akila Welihinda, Alan Hayes, Alec Radford, et al. Gpt-4o system card. *arXiv preprint arXiv:2410.21276*, 2024.
- Google Imagen 3 Team. Imagen 3. 2024. URL <https://arxiv.org/pdf/2408.07009>.
- Black Forest Labs. Flux. 2024. URL <https://github.com/black-forest-labs/flux>.
- Bin Lin, Zongjian Li, Xinhua Cheng, Yuwei Niu, Yang Ye, Xianyi He, Shenghai Yuan, Wangbo Yu, Shaodong Wang, Yunyang Ge, et al. Uniworld: High-resolution semantic encoders for unified visual understanding and generation. *arXiv preprint arXiv:2506.03147*, 2025.
- Yaron Lipman, Ricky TQ Chen, Heli Ben-Hamu, Maximilian Nickel, and Matt Le. Flow matching for generative modeling. *arXiv preprint arXiv:2210.02747*, 2022.
- Shiyu Liu, Yucheng Han, Peng Xing, Fukun Yin, Rui Wang, Wei Cheng, Jiaqi Liao, Yingming Wang, Honghao Fu, Chunrui Han, et al. Step1x-edit: A practical framework for general image editing. *arXiv preprint arXiv:2504.17761*, 2025.
- Yuan Liu, Haodong Duan, Yuanhan Zhang, Bo Li, Songyang Zhang, Wangbo Zhao, Yike Yuan, Jiaqi Wang, Conghui He, Ziwei Liu, et al. Mmbench: Is your multi-modal model an all-around player? In *European conference on computer vision*, pp. 216–233. Springer, 2024.
- Xichen Pan, Satya Narayan Shukla, Aashu Singh, Zhuokai Zhao, Shlok Kumar Mishra, Jialiang Wang, Zhiyang Xu, Jiu hai Chen, Kunpeng Li, Felix Juefei-Xu, et al. Transfer between modalities with metaqueries. *arXiv preprint arXiv:2504.06256*, 2025.
- Dustin Podell, Zion English, Kyle Lacey, Andreas Blattmann, Tim Dockhorn, Jonas Müller, Joe Penna, and Robin Rombach. Sdxl: Improving latent diffusion models for high-resolution image synthesis. *arXiv preprint arXiv:2307.01952*, 2023.
- Aditya Ramesh, Prafulla Dhariwal, Alex Nichol, Casey Chu, and Mark Chen. Hierarchical text-conditional image generation with clip latents. *arXiv preprint arXiv:2204.06125*, 1(2):3, 2022.
- Robin Rombach, Andreas Blattmann, Dominik Lorenz, Patrick Esser, and Björn Ommer. High-resolution image synthesis with latent diffusion models. In *Proceedings of the IEEE/CVF conference on computer vision and pattern recognition*, pp. 10684–10695, 2022.
- Weijia Shi, Xiaochuang Han, Chunting Zhou, Weixin Liang, Xi Victoria Lin, Luke Zettlemoyer, and Lili Yu. Lmfusion: Adapting pretrained language models for multimodal generation. *arXiv preprint arXiv:2412.15188*, 2024.
- Jiaming Song, Chenlin Meng, and Stefano Ermon. Denoising diffusion implicit models. *arXiv preprint arXiv:2010.02502*, 2020.
- Zhenxiong Tan, Songhua Liu, Xingyi Yang, Qiaochu Xue, and Xinchao Wang. Ominicontrol: Minimal and universal control for diffusion transformer. 2023.
- Bingda Tang, Boyang Zheng, Sayak Paul, and Saining Xie. Exploring the deep fusion of large language models and diffusion transformers for text-to-image synthesis. In *Proceedings of the Computer Vision and Pattern Recognition Conference*, pp. 28586–28595, 2025.

- Chameleon Team. Chameleon: Mixed-modal early-fusion foundation models. *arXiv preprint arXiv:2405.09818*, 2024.
- Team Wan, Ang Wang, Baole Ai, Bin Wen, Chaojie Mao, Chen-Wei Xie, Di Chen, Fei Wu Yu, Haiming Zhao, Jianxiao Yang, Jianyuan Zeng, Jiayu Wang, Jingfeng Zhang, Jingren Zhou, Jinkai Wang, Jixuan Chen, Kai Zhu, Kang Zhao, Keyu Yan, Lianghua Huang, Mengyang Feng, Ningyi Zhang, Pandeng Li, Pingyu Wu, Ruihang Chu, Ruili Feng, Shiwei Zhang, Siyang Sun, Tao Fang, Tianxing Wang, Tianyi Gui, Tingyu Weng, Tong Shen, Wei Lin, Wei Wang, Wei Wang, Wenmeng Zhou, Wenten Wang, Wenting Shen, Wenyuan Yu, Xianzhong Shi, Xiaoming Huang, Xin Xu, Yan Kou, Yangyu Lv, Yifei Li, Yijing Liu, Yiming Wang, Yingya Zhang, Yitong Huang, Yong Li, You Wu, Yu Liu, Yulin Pan, Yun Zheng, Yuntao Hong, Yupeng Shi, Yutong Feng, Zeyinzi Jiang, Zhen Han, Zhi-Fan Wu, and Ziyu Liu. Wan: Open and advanced large-scale video generative models. *arXiv preprint arXiv:2503.20314*, 2025.
- Guo-Hua Wang, Shanshan Zhao, Xinjie Zhang, Liangfu Cao, Pengxin Zhan, Lunhao Duan, Shiyin Lu, Minghao Fu, Xiaohao Chen, Jianshan Zhao, et al. Ovis-u1 technical report. *arXiv preprint arXiv:2506.23044*, 2025a.
- Peiyu Wang, Yi Peng, Yimeng Gan, Liang Hu, Tianyidan Xie, Xiaokun Wang, Yichen Wei, Chuanxin Tang, Bo Zhu, Changshi Li, et al. Skywork unipic: Unified autoregressive modeling for visual understanding and generation. *arXiv preprint arXiv:2508.03320*, 2025b.
- Xinlong Wang, Xiaosong Zhang, Zhengxiong Luo, Quan Sun, Yufeng Cui, Jinsheng Wang, Fan Zhang, Yueze Wang, Zhen Li, Qiyong Yu, et al. Emu3: Next-token prediction is all you need. *arXiv preprint arXiv:2409.18869*, 2024.
- Yuhan Wang, Siwei Yang, Bingchen Zhao, Letian Zhang, Qing Liu, Yuyin Zhou, and Cihang Xie. Gpt-image-edit-1.5 m: A million-scale, gpt-generated image dataset. *arXiv preprint arXiv:2507.21033*, 2025c.
- Cong Wei, Zheyang Xiong, Weiming Ren, Xeron Du, Ge Zhang, and Wenhui Chen. Omniedit: Building image editing generalist models through specialist supervision. In *The Thirteenth International Conference on Learning Representations*, 2024.
- Hongyang Wei, Baixin Xu, Hongbo Liu, Cyrus Wu, Jie Liu, Yi Peng, Peiyu Wang, Zexiang Liu, Jingwen He, Yidan Xietian, et al. Skywork unipic 2.0: Building context model with online rl for unified multimodal model. *arXiv preprint arXiv:2509.04548*, 2025.
- Chengyue Wu, Xiaokang Chen, Zhiyu Wu, Yiyang Ma, Xingchao Liu, Zizheng Pan, Wen Liu, Zhenda Xie, Xingkai Yu, Chong Ruan, et al. Janus: Decoupling visual encoding for unified multimodal understanding and generation. In *Proceedings of the Computer Vision and Pattern Recognition Conference*, pp. 12966–12977, 2025a.
- Chenyuan Wu, Pengfei Zheng, Ruiran Yan, Shitao Xiao, Xin Luo, Yueze Wang, Wanli Li, Xiyan Jiang, Yexin Liu, Junjie Zhou, et al. Omnigen2: Exploration to advanced multimodal generation. *arXiv preprint arXiv:2506.18871*, 2025b.
- Shitao Xiao, Yueze Wang, Junjie Zhou, Huaying Yuan, Xingrun Xing, Ruiran Yan, Chaofan Li, Shuting Wang, Tiejun Huang, and Zheng Liu. Omnigen: Unified image generation. In *Proceedings of the Computer Vision and Pattern Recognition Conference*, pp. 13294–13304, 2025.
- Jinheng Xie, Weijia Mao, Zechen Bai, David Junhao Zhang, Weihao Wang, Kevin Qinghong Lin, Yuchao Gu, Zhijie Chen, Zhenheng Yang, and Mike Zheng Shou. Show-o: One single transformer to unify multimodal understanding and generation. *arXiv preprint arXiv:2408.12528*, 2024.
- Jinheng Xie, Zhenheng Yang, and Mike Zheng Shou. Show-o2: Improved native unified multimodal models. *arXiv preprint arXiv:2506.15564*, 2025.
- Yang Ye, Xianyi He, Zongjian Li, Bin Lin, Shenghai Yuan, Zhiyuan Yan, Bohan Hou, and Li Yuan. Imgedit: A unified image editing dataset and benchmark. *arXiv preprint arXiv:2505.20275*, 2025.
- Weihao Yu, Zhengyuan Yang, Linjie Li, Jianfeng Wang, Kevin Lin, Zicheng Liu, Xinchao Wang, and Lijuan Wang. Mm-vet: Evaluating large multimodal models for integrated capabilities. *arXiv preprint arXiv:2308.02490*, 2023.

Xiang Yue, Yuansheng Ni, Kai Zhang, Tianyu Zheng, Ruoqi Liu, Ge Zhang, Samuel Stevens, Dongfu Jiang, Weiming Ren, Yuxuan Sun, et al. Mmmu: A massive multi-discipline multimodal understanding and reasoning benchmark for expert agi. In *Proceedings of the IEEE/CVF Conference on Computer Vision and Pattern Recognition*, pp. 9556–9567, 2024.

Kai Zhang, Lingbo Mo, Wenhui Chen, Huan Sun, and Yu Su. Magicbrush: A manually annotated dataset for instruction-guided image editing. *Advances in Neural Information Processing Systems*, 36:31428–31449, 2023.

Zechuan Zhang, Ji Xie, Yu Lu, Zongxin Yang, and Yi Yang. In-context edit: Enabling instructional image editing with in-context generation in large scale diffusion transformer. *arXiv preprint arXiv:2504.20690*, 2025.

Chunting Zhou, Lili Yu, Arun Babu, Kushal Tirumala, Michihiro Yasunaga, Leonid Shamis, Jacob Kahn, Xuezhe Ma, Luke Zettlemoyer, and Omer Levy. Transfusion: Predict the next token and diffuse images with one multi-modal model. *arXiv preprint arXiv:2408.11039*, 2024.